Image Cover Sheet

CLASSIFICATION	SYSTEM NUMBER
UNCLASSIFIED	510033

TITLE

PULSED EDDY CURRENT METHOD DEVELOPMENTS FOR HIDDEN CORROSION DETECTION IN AIRCRAFT STRUCTURES

System Number:

Patron Number:

Requester:

Notes:

DSIS Use only:

Deliver to:

PULSED EDDY CURRENT METHOD DEVELOPMENTS FOR HIDDEN CORROSION DETECTION IN AIRCRAFT STRUCTURES

Provided by

Capt B.A. Lepine, Research and Development Officer, Air Vehicle Research Detachment, DND
B.P. Wallace, University of Victoria, Cooperative Student
D.S. Forsyth, Institute for Aerospace Research, National Research Council Canada (NRC/IAR)
A. Wyglinski, McGill University, Defence Research Assistant

Introduction

When assessing the condition of multi-layered aircraft structures using nondestructive testing (NDT), there is a requirement to accurately characterize hidden corrosion by identifying the affected layers, and measuring both the amount of metal loss and the associated pillowing due to the corrosion products. Such aircraft corrosion inspection systems require sensitive and discriminating NDT techniques. Also, reducing inspection times for large areas and simplifying inspection interpretation are increasingly important. Inspection systems must quickly acquire large amounts of information and be adaptable to automated scanning and imaging technologies. This paper investigates the pulsed eddy current method as an approach that addresses these requirements by examining its potential for detecting and characterizing corrosion in thin skin fuselage lap splices.

Background

Conventional eddy current NDT methods use single frequency sinusoidal excitation and measure flaw responses as impedance or voltage changes on an impedance plane display. Inspectors interpret the magnitude and phase changes to detect flaws, but they lack the information necessary to completely characterize a flaw. Multiple frequency measurements can be combined to more accurately assess the condition of a component by reducing signal anomalies that may otherwise mask the flaws. Some instruments feature frequency mixing functions that can quickly apply this principle in dual frequency methods. This approach has been shown to be useful in reducing the effects of plate separation variations when inspecting for second layer corrosion in lap splices [1]. Dual frequency methods are also advantageous when performing large area inspections by means of eddy current C-scans of specimens with corrosion under fasteners [2]. Unfortunately, conventional multiple frequency methods are limited by their inability to perform quantitative measurements. Also, it is difficult to generate visualisation of these data in an intuitive manner.

Swept frequency measurements using impedance analyzers perform well in quantitative corrosion characterization studies, especially when they are interpreted with theoretical models [3]. These techniques do not lend themselves to scanning methods, however, and are much too laborious for practical applications.

In contrast to conventional eddy current methods, pulsed eddy current (PEC) excites the probe's driving coil with a repetitive broadband pulse, such as a square wave. The resulting transient current through the

coil induces transient eddy currents in the test piece, associated with highly attenuated magnetic pulses propagating through the material. At each probe location, a series of voltage-time data pairs are produced as the induced field decays, analogous to ultrasonic inspection data.

Since a broad frequency spectrum is produced in one pulse, the reflected signal contains depth information of the material. Physically, the pulse is broadened and delayed as it travels deeper into the highly dispersive material. Therefore, flaws or other anomalies close to the surface will affect the eddy current response earlier in time than deep flaws.

The modes of presentation of PEC data are analogous to ultrasonic methods in the form of A-, B- and C-scans [4]. Interpretation, therefore, may be considered more intuitive than conventional eddy current data.

PEC methods are very flexible: The excitation pulse, signal gain and sensor configurations can be modified to suit particular applications.

These principles have been discussed in previous work [5],[6]. The specific application of PEC for characterizing hidden corrosion in aircraft structures has been a topic in several other publications on which a large part of this work is based [4],[6-9].

This paper will present the AVRD PEC system design, and the results of pulsed eddy current experiments performed on laboratory and in-service multi-layered specimens. The various ways of presenting PEC data will be illustrated, such as the time based A-scan spot measurements, the one-dimensional time-based B-scan and the 2-dimensional C-scan image formats. Several preliminary empirical interpretations are also presented; however, further experiments and modelling will be necessary before complete PEC data analysis is possible.

Pulsed Eddy Current System Setup

Figure 1 shows a schematic of the experimental setup designed to produce pulsed eddy current signals and measure the transients affected by flaws in scanned

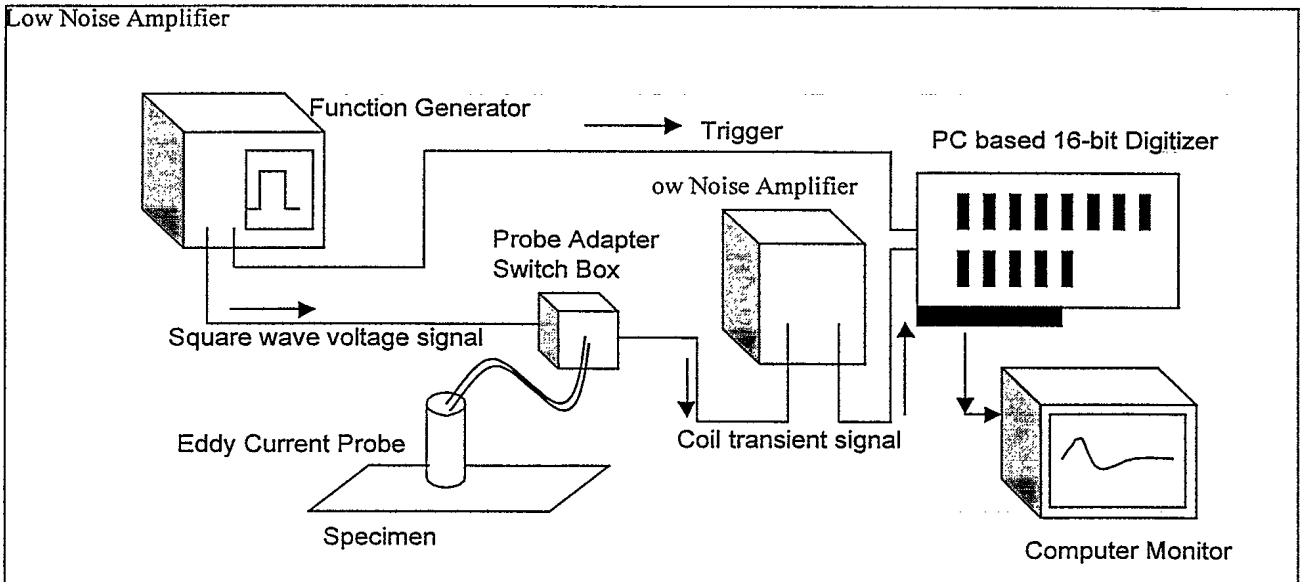

Figure 1 - The AVRD Pulsed Eddy Current System

specimens. This system was developed at the Air Vehicle Research Detachment, Department of National Defence, Ottawa.

The system is based on a technique initially developed by Moulder *et al.*[7], in which the signal is measured as the voltage drop across a resistor and fed into a low-noise amplifier, then digitized by a PC based data acquisition system. The Winspect™ software by Utex Scientific Instruments, Inc. was used to acquire the data and display the signals in the form of A-, B-, or C-scans. Further signal analysis and processing was performed using NDI Analysis, a software package developed at NRC/IAR.

The system can accommodate several probe-coil configurations: (i) a single absolute coil that both drives and receives the EM field transients; (ii) a two coil arrangement where each coil can be switched to function as either driver or pick-up; and (iii) a differential set up where one stationary coil rests on a reference standard and the other moves across a test specimen. Three probes were used for all the tests described in this paper: (a) a single air-core coil for setup (i), (b) a "stacked" driver/pick-up (D/P) probe with one air-core coil above another identical coil for setup (ii), and (c) another D/P probe with a smaller 1.6mm diameter ferrite-core receive coil located co-axially within the drive coil. All probes have a 14mm outer diameter driver coil, and probe (c) has a 6.35mm outer diameter pickup coil. As a first approximation, the probes were designed to operate with a centre frequency of 12kHz. The manufacturer supplied the probe design parameters for future modelling and optimized design work.

The flexibility in the system is achieved through a Probe Adapter Switch Box to select the mode of operation and the resistor across which the signal is measured. There is also a wide range of gain settings on the received signal amplifier from 1X to 50,000X. The drive voltage, ranging from 1 to 30 volts, and the waveform shapes are modified easily on the function generator. All the settings in the system depend heavily on the parameters of the probes in use and the specimens under test.

Specimens

Calibration test specimens were constructed from 1 mm thick 2024-T3 aluminum alloy sheets commonly used for aircraft fuselage skin structures. One 100 mm x 300 mm sheet had six 25 mm wide strips milled to various depths from 0.05 mm (5%) to 0.46 mm (46%) deep. This sheet was placed atop another unflawed sheet to simulate thinning on the bottom side of the first layer due to corrosion. By inverting this combination, the specimen simulates thinning on the top of the second layer. A variable gap between two intact layers was represented by a steadily increasing number of paper strips between the metal sheets to simulate the presence of a scrim cloth or corrosion products. A similar approach was taken to simulate varying lift-off distances from the probe to the surface. All gaps, milled areas and sheet thickness were measured with a micrometer.

The second specimen type consisted of a sample removed from a retired Boeing 727 fuselage lap splice containing hidden natural corrosion. This sample's skin structure consisted of two 1.27 mm thick 2024-T3 Al sheets, along with a stringer.

Experimental Procedure

The function generator was used to produce a simple 1 kHz bipolar square wave throughout the entire range of tests. The received signal was recorded at 16 bits

precision with a 1 MHz sampling rate. The first half of the periodic signal was recorded at every point. An automated scanning table was used to move the specimens in a raster pattern with the probe held in place. This produced area scans from 7500 to 15000 mm^2 per specimen in about 3-5 minutes each. The signals were not averaged since the data was captured during relatively fast area scans.

A single reference signal was chosen at a position where the material was known to have no flaws and consist of only the two 1mm thick metal sheets. Using the functions provided by Winspect™ and/or NDI Analysis, the reference signal was subtracted from those at the remaining points of the scan, resulting in a set of reference subtracted signals, also called A-scans. These represent the perturbations due to flaws or other abnormal conditions. B-scans and C-scans were extracted from the data by using time gating and feature collapse functions on the A-scan data.

Results and Discussion

The calibration specimens were scanned first with all three probes and the results stored in digital format using Winspect ™. Scanning calibration specimens allows one to view the effects of known structural changes such as thinning and substructure. Although all the probes had some measure of success in detecting the various amounts of thinning, probe (c) produced the strongest flaw transient responses and provided the most resolution due to its smaller pick-up coil. Only the results from probe (c) are given in this paper.

A-scans

Figure 2 shows the transient signals measured by the pick-up coil for various typical test parameters and/or material conditions. Since the signal is a voltage measured across a resistor in series with the coil, the curves can be considered as relative measurements of the current induced into the coil in reaction to the changing magnetic fields at the surface of the material. These signals, therefore, contain the total information on both the incident and reflected fields. It is immediately apparent that the signals undergo only very subtle shape and amplitude changes, even for extremely different test conditions.

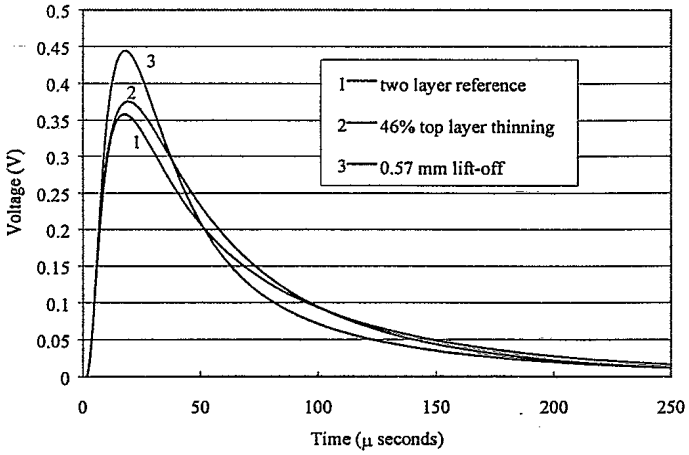

Figure 2 - Transient signals measured by the pick-up coil for three different test parameters

The reference subtracted A-scans are found in Figure 3. Features can be seen in these flaw response signals that may help to characterize certain flaw parameters, such as the affected layer, its depth and percent metal loss. The signal's amplitude and its time-to-zero-crossing (TZC) are the two most prominent features affected by these parameters.[7]

The results found by Moulder *et al.* [7] have been reproduced in these experiments to show the distinctive features of the A-scans and to illustrate their potential for discriminating against the different locations of the thinning. As expected, thinning in the first layer has earlier TZC than second layer

thinning. Furthermore, larger amounts of thinning in the first layer cause the signals to have earlier TZCs because their metal/air interfaces are progressively closer to the surface. In contrast, second layer metal loss does not have a moving metal/air interface, thus its TZC remains relatively stable for all sizes.

While scanning any typical aircraft component, one will eventually encounter several structural variances not associated with corrosion or other flaws, making the inspection more complex. For example, PEC signals are extremely sensitive to the smallest amounts of plate separation that may not be attributed to corrosion. These "benign" air gaps are encountered in real aircraft components due to scrim cloths, and minor bulging or warping around rivets. Another common noise source is the constant variation in the lift-off distance between the probe face and the surface. Lastly, substructure changes such as metal thickness increase due to the encounter of stringers also affect the signals differently.

Each of these test condition variations is illustrated in Figure 4. Lift-off signals are shown to exhibit the earliest TZCs and largest amplitudes. The signal for the increasing metal thickness has a distinct inverted shape. Note that on their own, they have their distinct features, such as the differing TZCs; however, when these anomalies occur simultaneously, the analysis and interpretation becomes increasingly complex. Distinguishing between them by comparing and contrasting their relative signal features is extremely difficult. Preliminary experiments have revealed that when any of these anomalies are combined with thinning, the previously calibrated flaw signals of Figure 3 shift earlier in time. Closer investigation into their combinations is required before a more reliable and systematic approach can be used to distinguish between these co-existing features.

C-scans

After selecting the type of information to collapse from an A-scan, it is extremely useful to view the data in an image format called a C-scan. Time gates can be used to select certain portions of the A-scan data for analysis; for example, a C-scan image of the TZC can be generated for a portion of the A-scan which corresponds to a range of depth in the specimen.

Figure 5 illustrates an amplitude C-scan for the calibrated specimen with thinning in the bottom of the first layer and top of the second layer. Clearly, these scans reveal that the PEC system can detect levels of corrosion as low as 5% of the single layer thickness. The depth information is provided by the TZC C-scans in Figures 6 and 7, with the former gated earlier in time than the latter. It is readily apparent from these scans that the flaws located in the top layer can be distinguished from those in the second layer. Note that the TZCs seen in Figure 6(b) were likely due to a small amount of plate separation. Also, when the signal is very small, the noise fluctuations can cross the zero axis several times, often causing the TZCs C-scans to be noisy.

B-scans

B-scans of the same calibration samples, given in Figure 8, display a linear cross section through a C-scan, with time as the domain and the signal amplitude presented in greyscale. The interpretation of this data can be deceiving, but when done properly, the time scale can be closely associated with depth information. Hence, the illustrated B-scans, extracted from the C-scans of Figures

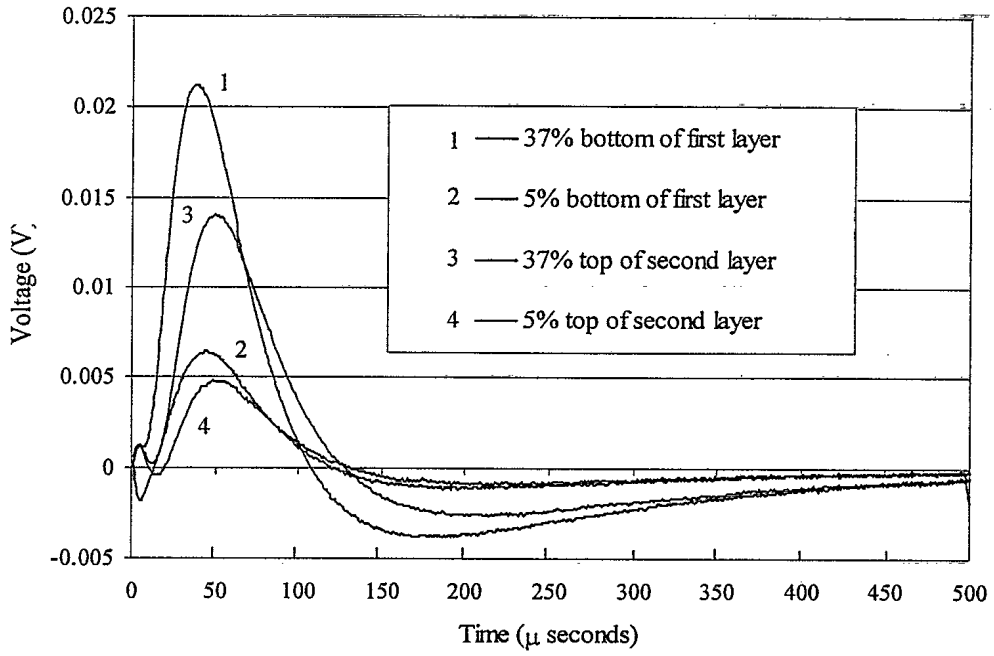

Figure 3 - A-scans representing flaw transients due to metal loss in the two layered calibration specimens

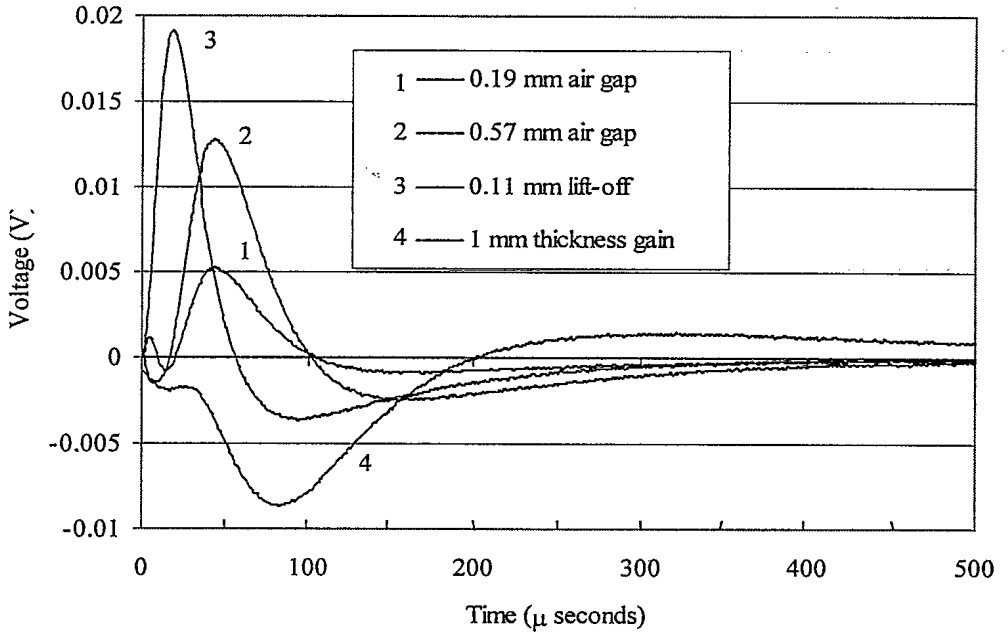

Figure 4 - A-scans representing transients forced by other variances in the calibration specimens or test parameters

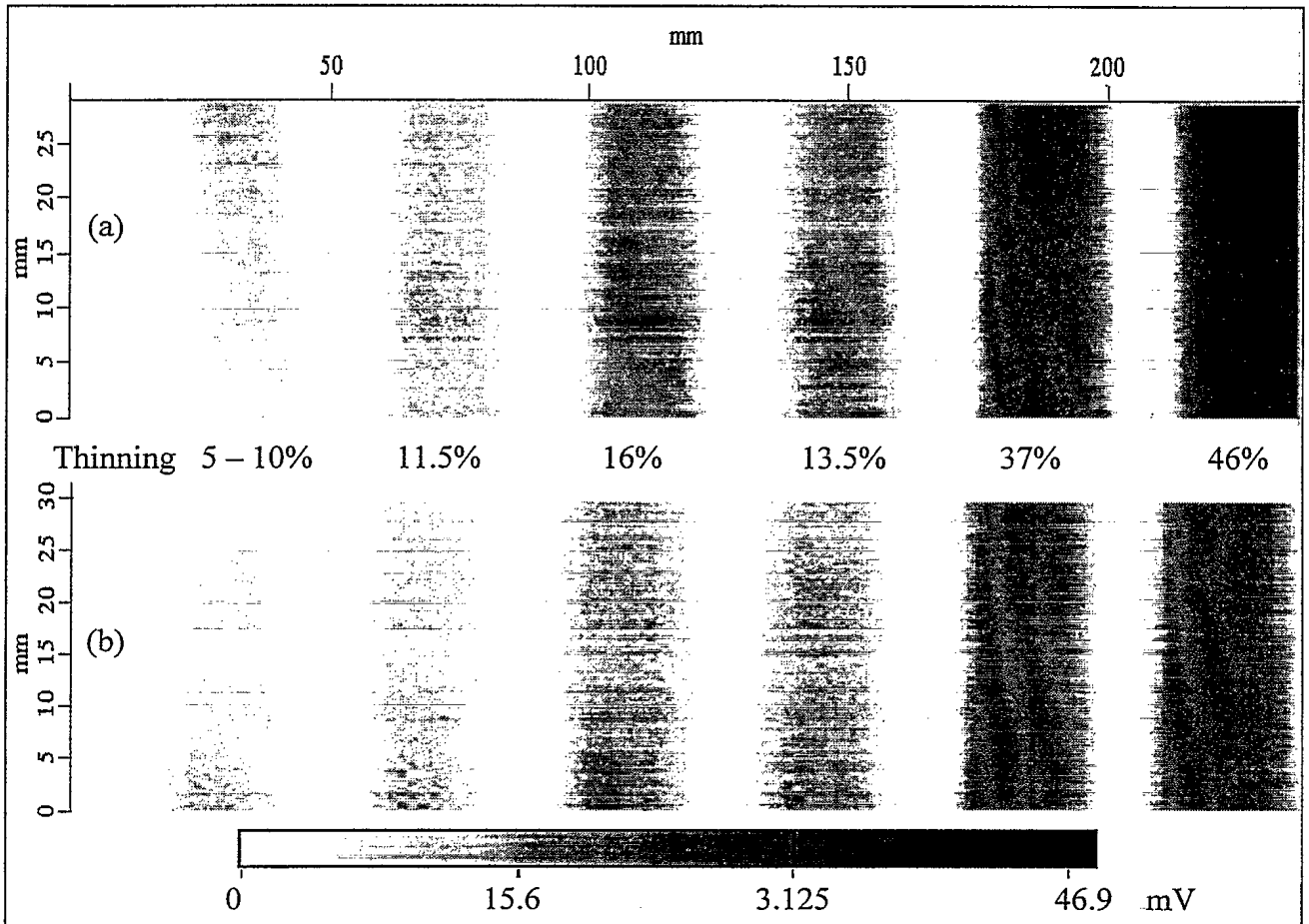

Figure 5 - PEC amplitude c-scan of the calibration specimens with metal loss located (a) in the bottom of the first layer and (b) at the top of the second layer

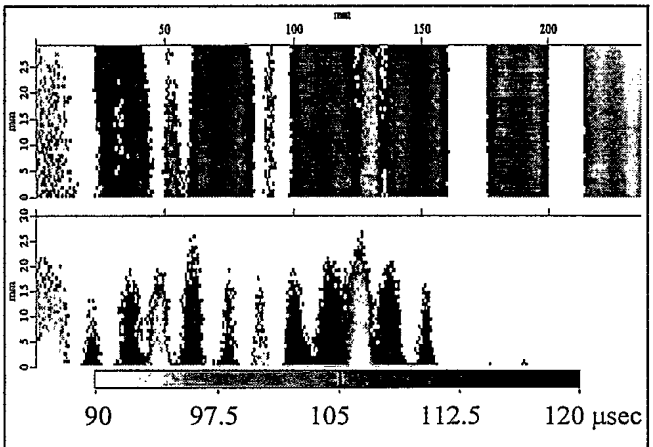

Figure 6 - Early time-to-zero-crossing c-scan of specimens (a) and (b) in Figure 5

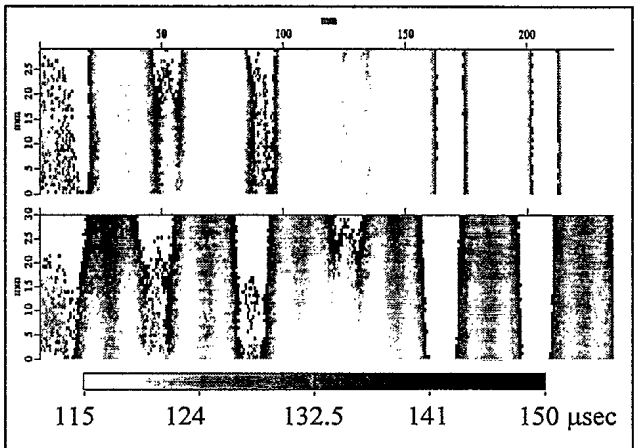

Figure 7 - Late time-to-zero-crossing c-scan of specimens (a) and (b) in Figure 5

6 and 7, provide an alternative means of distinguishing between first layer and second layer thinning. In this case, the TZC at each position is marked to show its shift related to the depth of the flaws.

The corroded specimen was scanned using the same probe and experimental settings as before. Note that since the wall thickness for the corroded specimen is larger than the calibration specimen, it will have slightly different amplitude responses to that of the calibration sample for the same size flaw. A second set of calibration samples would be required to infer metal loss and depth more accurately. This issue notwithstanding, the amplitude C-scan image of Figure 9 reveals a region of intense corrosion activity. The TZC C-scan in Figure 10 is more cluttered. As expected, however, the TZCs in the corroded region are much earlier due to the stringer through the centre row of rivets than at locations away from the stringer. Further interpretation was not attempted since the combinations of flaw, sub-structural variations, and test parameters such as lift-off occur randomly throughout the scan.

It has been shown how certain signal features are affected by different specimen features or test parameters. However, it is obvious that these features can be very difficult to separate out since the basic PEC A-scan signal shape changes little. The C-scans are also difficult to interpret, as evidenced by the corrosion scan in Figures 9 and 10. Hence, there needs to be a more intuitive way of visualising the signals so that certain obvious features can be clearly separated, as is done for lift-off signals on the impedance plane in conventional eddy current, for example. In addition, although the human brain may be incapable of effectively interpreting visually similar signals, the information contained in the PEC signals is vast and more information may be retrievable with modern computing methods.

Conclusions

It has been demonstrated that PEC has very high potential for applications in corrosion detection and characterization. Its most powerful advantage over conventional eddy current is the ability to capture broadband frequency information within a single transient signal. Consequently, when analyzed properly, PEC scans contain valuable depth information essential for characterizing corrosion in aircraft structures. The time-based signals are more intuitive and can be displayed in various formats presently used in ultrasonic NDT. The A-, B- and C-scans function well as complimentary methods for presenting data when simple variations in test parameters occur; these displays can become very complex and confusing, however, when combinations of such variations occur simultaneously.

The PEC system demonstrated a sensitivity of at least 5% total metal loss, or 0.05 mm thinning, in the second layer. Smaller levels of corrosion and deeper penetration may be achieved with optimized probe designs and test parameters, such as excitation current shape and frequencies.

Two of the most problematic test parameters to control are probe lift-off and specimen layer separations. Simply gating out transient responses with early zero-crossings for such anomalies also removes the flaw information. A new concept of visualising the data is required to separate out such signals when they occur simultaneously over genuine flaws. For example, a method may be developed to separate lift-off from flaw signals, as is now performed in conventional eddy current. These noise sources, flaws,

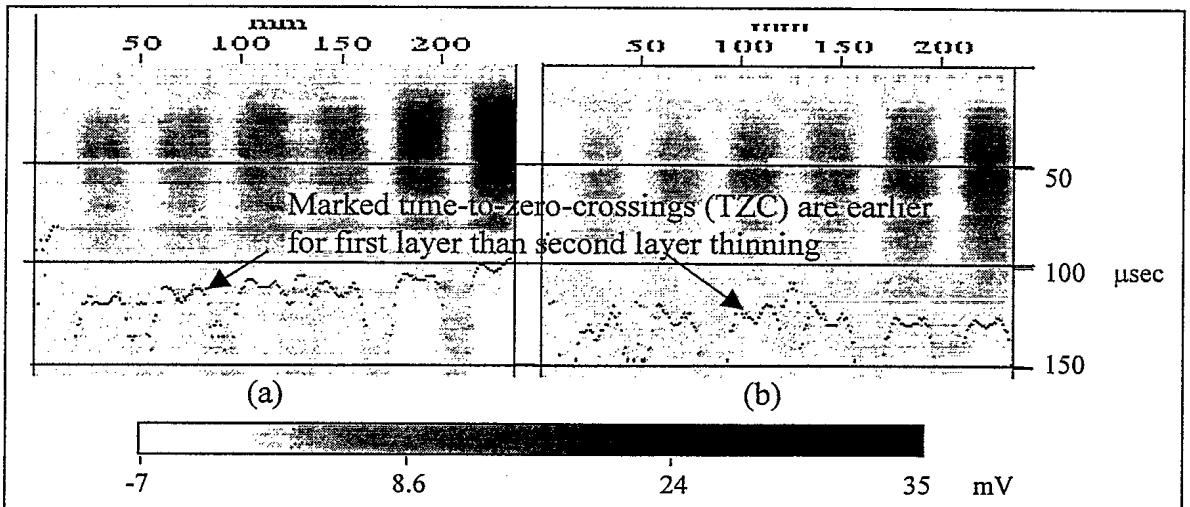

Figure 8 - B-scans taken at the 15mm position of specimens (a) and (b) in Figure 5

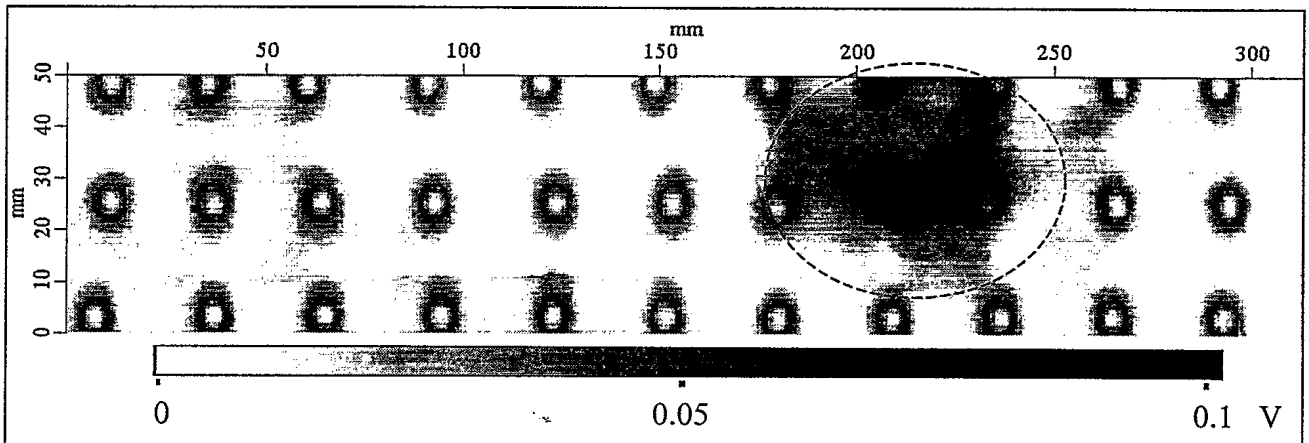

Figure 9 - Amplitude c-scan of Boeing 727 fuselage lap splice with natural corrosion

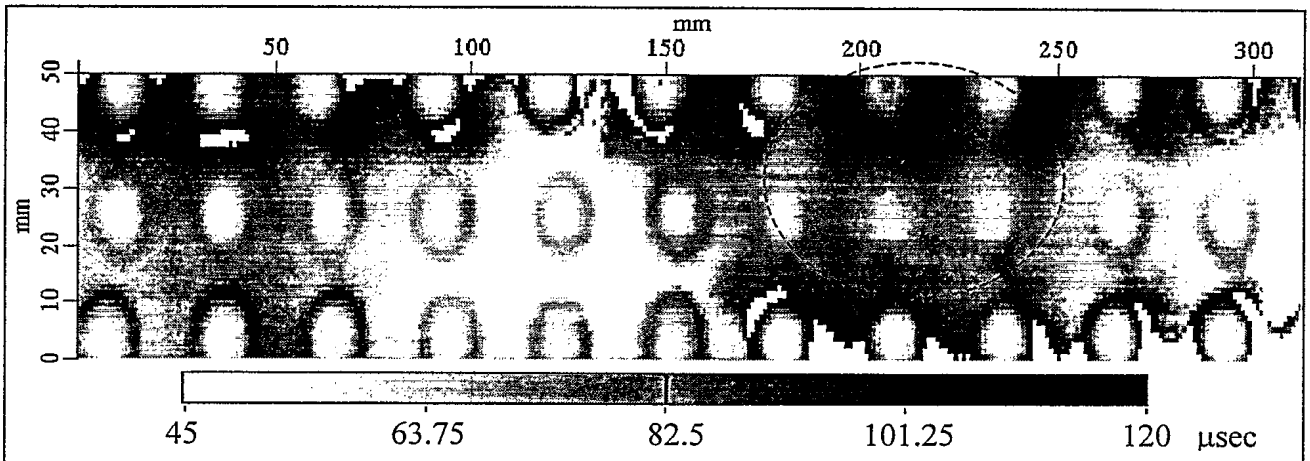

Figure 10 - Time-to-zero-crossing c-scan of Boeing 727 specimen in Figure 9

and other test parameter variations were shown to exhibit distinct features when analyzed separately without the interference from each other, thus offering some potential means of separating their responses in future work.

Future Work

It is evident from the tests and analyses performed in this study that PEC is not a completely mature NDT technology. Its distinctive signal features need to be studied experimentally and theoretically to completely understand and properly interpret the results.

The unique PEC signal features for common anomalies and test parameter variations will be combined and analyzed using advanced signal processing programs such as NRC's NDI Analysis. The application of three dimensional Finite Element Modelling of the EM fields using a transient solver is also planned as an important step towards interpreting these features, and identifying new ones. It is hoped that such an approach will lead to ways of separating out the effects from different test parameters, such as lift-off and air gaps between the layers to distinguish them from volume loss in the material, as well as develop a quantitative or absolute methods of measuring flaws.

Lastly, similar experiments will be performed on thicker materials, such as that found on wing skin structures. In these cases, significant depth penetration and flaw depth information is required, hence, pulsed eddy current methods are ideal. However, as the lower frequency components become more important, coils used as field sensors may be less effective since their signal magnitudes are proportional to the rate of change of the magnetic flux. Consequently, sensors that measure the magnetic field strength will be required and applied for these tests.

Acknowledgements

Thanks are due to Eddytech for constructing the coils used in this work and providing their specifications. The authors are also grateful to Mr. Ron Gould at NRC/IAR for preparing the corrosion specimen.

References

[1] J.G. Thompson, "Subsurface Corrosion Detection in Aircraft Lap Splices Using a Dual Frequency Eddy Current Inspection Technique", Materials Evaluation, December 1993, pp 1398-1401.

[2] B.A. Lepine and R.T. Holt, "An Eddy Current Scanning Method for the Detection of Corrosion Under Fasteners in Thick Skin Aircraft Structures", Canadian Aeronautics and Space Journal, March 1997, pp28-33.

[3] S. Mitra, E. Uzal, J.H. Rose, J.C. Moulder, "Eddy Current Measurements of Corrosion-Related Thinning in Aluminum Lap Splices", Review of Progress in Quantitative Nondestructive Evaluation, Vol.12, 1993, pp 2003-2010.

[4] J.A. Bieber, C. Tai, J.C. Moulder, "Quantitative Assessment of Corrosion in Aircraft Structures Using Scanning Pulsed Eddy Current", Review of Progress in QNDE, Vol. 17, 1998, p 315.

[5] D.J. Harrison, "Progress in the Detection of Cracks Under Installed Fasteners Using Eddy Currents", Defence Research Agency Technical Report 91024, RAE, Farnborough UK, April 1991.

[6] D.J. Harrison, "Eddy Current Inspection Using Hall Sensors and Transient Excitation", Defence Research Agency Technical Report DRA/SMC/TR941008, DRA, Farnborough UK, June 1995.

[7] J.C. Moulder, M.W. Kubovich, E. Uzal, J.H. Rose, "Pulsed Eddy Current Measurements of Corrosion Induced Metal Loss: Theory and Experiment", Review of Progress in QNDE, Vol.14, 1995, p 2065.

[8] J.A. Bieber, S.K. Shaligram, J.H. Rose, J.C. Moulder, "Time-gating of Pulsed Eddy Current Signals for Defect Characterization and Discrimination in Aircraft Lap-Joints", Review of Progress in QNDE, Vol. 16, 1997, p 1915.

[9] S.K. Burke, G.R. Hugo, D.J. Harrison, "Transient Eddy-current NDE for Hidden Corrosion in Multilayer Structures", Review of Progress in QNDE, Vol. 17, 1998, p 307.

510033